BIK1, a Protein Required for Microtubule Function during Mating and Mitosis in *Saccharomyces cerevisiae*, Colocalizes with Tubulin

Vivian Berlin,* Cora A. Styles,* and Gerald R. Fink*‡

*Whitehead Institute for Biomedical Research and ‡Massachusetts Institute of Technology, Cambridge, Massachusetts 02142

Abstract. *BIK1* function is required for nuclear fusion, chromosome disjunction, and nuclear segregation during mitosis. The BIK1 protein colocalizes with tubulin to the spindle pole body and mitotic spindle. Synthetic lethality observed in double mutant strains containing a mutation in the *BIK1* gene and in the gene for α- or β-tubulin is consistent with a physical interaction between BIK1 and tubulin. Furthermore, over- or underexpression of BIK1 causes aberrant microtubule assembly and function. *bik1* null mutants are viable but contain very short or undetectable cytoplasmic microtubules. Spindle formation often occurs strictly within the mother cell, probably accounting for the many multinucleate and anucleate *bik1* cells. Elevated levels of chromosome loss in *bik1* cells are indicative of defective spindle function. Nuclear fusion is blocked in *bik1* × *bik1* zygotes, which have truncated cytoplasmic microtubules. Cells overexpressing *BIK1* initially have abnormally short or nonexistent spindle microtubules and long cytoplasmic microtubules. Subsequently, cells lose all microtubule structures, coincident with the arrest of division. Based on these results, we propose that BIK1 is required stoichiometrically for the formation or stabilization of microtubules during mitosis and for spindle pole body fusion during conjugation.

EVIDENCE obtained from biochemical experiments suggests that the key to the diverse functions of microtubules lies in the proteins associated with the microtubules. These proteins are thought to modulate the assembly and stability of microtubules and to mediate the interaction of microtubules with other cellular components. A number of proteins have been shown to coassemble with microtubules in vitro (reviewed by Olmsted, 1986) and associate with interphase and spindle microtubules (Vallee and Bloom, 1983; Bloom et al., 1984). Since most of the studies of microtubule-associated proteins (MAPs)[1] have been conducted in systems not amenable to genetic analysis, the in vivo functions of these MAPs are still uncertain. For this reason, recent interest has focused on microtubule function in yeast, where genetic interactions between tubulin and MAPs can be established.

In yeast, microtubules polymerize from a microtubule-organizing center, called the spindle pole body, which is embedded in the nuclear envelope. Microtubules emanate from the spindle pole body into the nucleus to form the spindle and out of the nucleus to form cytoplasmic microtubule arrays. The nuclear envelope in yeast remains intact throughout the mitotic cycle (Byers, 1981), effectively isolating the intranuclear and extranuclear microtubules.

Yeast has two functionally interchangeable genes for α-tubulin (Schatz et al., 1986*a*,*b*) and one for β-tubulin (Neff et al., 1983). Recent studies indicate that the tubulins are intimately involved in nuclear function. Mutations in the genes for α- and β-tubulin or drugs that depolymerize microtubules cause a block in mitosis, chromosome instability, inhibition of nuclear migration, and a block in nuclear fusion during zygote formation (Quinlan et al., 1980; Delgado and Conde, 1984; Thomas et al., 1985; Schatz et al., 1986b, 1988; Huffaker et al., 1988; Stearns and Botstein, 1988; Jacobs et al., 1988).

Genes for putative MAPs in yeast have been identified by isolating mutations in genes, other than those encoding the tubulins, which lead to defects in microtubule function. For example, genes affecting spindle function have been isolated by screening for mutants that exhibit high levels of chromosome loss during mitosis (Hieter et al., 1985; Meeks-Wagner et al., 1986; Hoyt et al., 1990). Among these are the *CIN1*, *CIN2*, and *CIN4* genes, which interact genetically with the α- or β-tubulin genes (Hoyt et al., 1990; Stearns et al., 1990). Another approach to microtubule function has been to isolate mutants blocked in nuclear fusion (Conde and Fink, 1976; Polaina and Conde, 1982), a process thought to involve cytoplasmic microtubules. These mutations define *KAR1*, which is implicated in spindle pole body function

Dr. Berlin's current address is Vertex Pharmaceuticals, 40 Allston Street, Cambridge, MA 02139.

1. *Abbreviations used in this paper*: DAPI, 4'-6-diamino-2-phenylindole; MAP, microtubule-associated proteins; PI, protease inhibitors; SC, synthetic medium; SD, minimal medium; YPD, rich medium.

(Rose and Fink, 1987), *KAR2*, the yeast homologue of mammalian Bip/GRP78 (Rose et al., 1989), and *KAR3*, which shows homology to the microtubule motor protein kinesin (Meluh and Rose, 1990). Despite the facility with which mutations can be obtained in genes affecting microtubule function, direct biochemical evidence for a physical interaction between the tubulins and the product of any of the genes defined by these mutations has been difficult to obtain, due in part to the low abundance of these proteins. Recently a mutant form of KAR3 and a KAR3-LacZ fusion protein have been localized by immunofluorescence to the cytoplasmic microtubules (Meluh and Rose, 1990).

In this paper, we show that *BIK1* is required for microtubule-mediated events on the basis of genetic experiments, and that the BIK1 protein co-localizes with tubulin as determined by indirect immunofluorescence. The *bik1-518* mutation was originally shown to cause a bilateral karyogamy defect (Trueheart et al., 1987). We now show that *bik1* null mutants, although viable, exhibit altered microtubule assembly, function, and localization. BIK1 colocalizes with the spindle pole body in unbudded cells just prior to bud emergence. Overexpression of *BIK1* results in the disappearance of microtubule structures and the arrest of cell division. Structural similarities between BIK1 and the mammalian MAP, tau, implicate the amino terminus of BIK1 in microtubule binding and suggest, together with our other results, that BIK1 associates directly with tubulin, regulating the assembly or stabilization of microtubules during the cell cycle.

Materials and Methods

Plasmids

The plasmids used in this work are listed in Table I. Ligations were performed in low-melting point agarose (Struhl, 1983) using 89 mM Tris-borate, 89 mM boric acid, and 10 mM EDTA, pH 8.0, as the electrophoresis buffer. Other DNA manipulations were performed as described by Maniatis et al. (1982). The plasmid pVB19 was propagated in *Escherichia coli* strain TG1 (Carter et al., 1985). *E. coli* strain LE392 (Borck et al., 1976) was used for all other transformations.

Strain Construction and Growth Conditions

Yeast strains used in this work are listed in Table II. Rich medium (YPD), minimal medium (SD), synthetic complete medium (SC), yeast cell culture, and tetrad analysis were as described by Sherman et al., (1986). All yeast transformations were carried out by the lithium acetate method of Ito et al., (1983). The *bik1-1::TRP1* allele was constructed by single step disruption (Rothstein, 1983) by transforming the *BIK1* parents of S/B 506 and L4324 with a 3.3-kb Sna BI plus Eco RI digest of pVB17, which contained a *TRP1* marked *BIK1* disruption. Trp+ prototrophs were selected and allele replacement was confirmed by Southern analysis (Southern, 1975). The *bik1-518* mutation, constructed by linker insertion mutagenesis, is a frameshift mutation at amino acid 183 and has been described (Trueheart et al., 1987).

*MAT*a/*MAT*a strains were constructed by transforming *MAT*a/*MAT*α strains with the GAL-HO plasmid pSB283, as described (Berlin et al., 1990). The resulting *MAT*a/*MAT*a strains were cured of pSB283 by growth of the strains on YPD.

Immunofluorescence Microscopy

Immunofluorescent staining of yeast cells was performed using a modification of the methods of Adams and Pringle (1984). Cells were fixed in 3.7% formaldehyde in 0.1 M KPO_4, pH 6.5 for 90 min at room temperature. Subsequent antibody incubations and washes were performed in 0.1 M KPO_4, pH 7.5, 1.2 M sorbitol. Cells were applied to the wells of multiwell microscope slides (Cel-Line, Newfield, NJ) treated with 1% polyethylenimine (Sigma Chemical Co., St. Louis, MO). Antibody incubations were performed for 1 h at room temperature. For double-labeling experiments, cells were incubated simultaneously with anti-BIK1 and anti-tubulin antibodies for 1 h and sequentially with the secondary antibodies, each for 1 h. Cells were examined with a Zeiss Axioskop equipped for epifluorescence microscopy and photographed on hypersensitized Technical Pan 2415 (Lumicon, Livermore, CA).

The primary antibodies used for immunofluorescence experiments were anti-BIK1 antibody diluted 1/20; YOL1/34 (Kilmartin et al., 1982), a rat mAb directed against α-tubulin (Sera-lab, Sussex, England) diluted 1/50; 206.1, a rabbit polyclonal antibody directed against β-tubulin diluted 1/1,000. 206.1 was kindly provided by Frank Solomon (Massachusetts Institute of Technology). Secondary antibodies were FITC-conjugated, affinity-purified donkey anti-rabbit IgG diluted 1/50 and Texas Red-conjugated, affinity purified goat anti-rat IgG diluted 1/400 (Jackson Immunoresearch Laboratories, Inc., West Grove, PA).

4',6-Diamino-2-phenylindole (DAPI) Staining of DNA

Cells fixed with 3.7% formaldehyde and permeabilized with 0.1% Triton-X-100 or fixed with methanol/acetic acid (3:1) were stained with DAPI as described previously (Berlin et al., 1990).

Table I. Plasmids

Plasmids	Description
pGN622	
VB100	The Hind III site in the 2 micron-plasmid DNA of pGN622 (unpublished results) was filled in using the Klenow fragment of DNA polymerase I, generating a plasmid with a unique Hind III site between the ampicillin and tetracycline resistance genes.
pVB16	A 3-kb Hind III–Eco RI fragment containing the *BIK1* gene was cloned into the Hind III and Eco RI sites of pUC19 (Yanisch-Perron et al., 1985).
pVB20	The Hind III–Eco RI fragment from pVB16 was cloned into the Hind III and Eco RI sites of pVB100.
pVB17	A 852-bp blunt-ended Bgl II–Eco RI fragment containing the *TRP1* gene replaced the 237-bp Eco RV fragment of the *BIK1* gene (from amino acid 4 to 82) in pVB16.
pDAD2	A polylinker was cloned into the Bam HI site of pCGS109 (provided by J. Schaum and J. Mao [Collaborative Research, Waltham, MA]) 3′ to the *GAL1* promoter.
pVB24	A 1.9-kb NcoI–Hind III fragment containing the *BIK1* gene was cloned into the Pvu II and Hind III sites of pDAD2 after filling in the Nco I site using the Klenow fragment of DNA polymerase I.
pVB19	A 720-bp Bgl II-Nsi I fragment of the *BIK1* gene encoding amino acids 101 to 340 was cloned into the Bam HI and Pst I sites of pATH11 (Koerner et al., 1990) generating an in-frame fusion of the *E. coli trpE* gene and *BIK1*.
pRS314	A *TRP1 CEN6* plasmid (Sikorski and Hieter, 1989) was kindly provided by P. Hieter (Johns Hopkins University).
pSB283	A *GAL-HO* plasmid containing *URA3* and *LEU2* (constructed by J. Trueheart; Berlin et al., 1990).
pRB327	*TUB1 LEU2 2μ* (Schatz et al., 1986*b*).
pRB1171	*CIN1 URA3 2μ*, kindly provided by Tim Stearns.

Table II. Strains

Strain	Genotype
L2736	*MATα ura3-52 leu2-3,112 his4-34* (J. Trueheart)
L2751	*MATα ura3-52 leu2-3,112 bik1-518* (J. Trueheart)
L2753	*MAT***a** *lys2 leu 2 kar1-1 bik1-518* (J. Trueheart)
L2964	*MAT***a** *ura3 leu1 ade2 can1 cyh2* [rho°] (J. Trueheart)
L2965	*MAT***a** *ura3 ade2 can1 cyh2 kar1-1* [rho°] (J. Trueheart)
L3758	*MAT***a** *ade2 his3Δ200 leu2-3, lys2Δ201 trp1Δ1 ura3-52 can1 cyh2*
L3762	*MAT***a** *ade2 his3Δ200 leu2-3,112 lys2Δ201 trp1Δ1 ura3-52 can1 cyh2 bik1-1::TRP1*
L3763	*MATα ade2 his3Δ200 leu2-3,112 lys2Δ201 trp1Δ1 ura3-52 can1 cyh2 bik1-1::TRP1*
L4320	*MAT***a**/*MAT***a** *ura3-52/ura3-52 leu2-3,112/leu2-3,112 trp1Δ1/trp1Δ1 lys2-201/lys2-201 his3Δ200/his3Δ200 ade2/ade2 cyh2/cyh2 can1/can1*
L4324	*MAT***a**/*MAT***a** *bik1-1::TRP1/bik1-1::TRP1 ura3-52/ura3-52 leu2-3,112/leu2-3,112 trp1Δ1/trp1Δ1 lys2-201/lys2-201 his3Δ200/his3Δ200 ade2/ade2 cyh2/cyh2 can1/can1* (isogenic with L4320)
L4392	*MAT***a**/*MATα ura3-52/ura3-52 leu2-3,112/leu2-3,112 ade2-101/+ his3Δ200/+ +/bik1-518 tub1-1/+*
L4393	*MAT***a**/*MATα ura3-52/ura3-52 his4/+ +/leu2-3,112 +/bik1-518 tub2-105/+*
L4394	*MAT***a**/*MATα ura3-52/ura3-52 lys2-801/+ his4-539/+ +/leu2-3,112 +/bik1-518 tub2-401/+*
L4395	MAT**a**/*MATα ura3-52/ura3-52 lys2-801/+ his4-539/+ +/leu2-3,112 +/bik1-518 tub2-403/+*
L4396	*MAT***a**/*MATα ura3-52/ura3-52 lys2-801/+ his4-539/+ +/leu2-3,112 +/bik1-518 tub2-404/+*
L4397	*MAT***a**/*MATα ura3-52/ura3-52 lys2-801/+ his4-539/+ +/leu2-3,112 +/bik1-518 tub2-405/+*
L4398	*MAT***a**/*MATα ura3-52/ura3-52 his4/+ +/leu2-3,112 +/bik1-518 tub2-104/+*

continued

Table II. (continued)

Strain	Genotype
L4399	*MAT***a**/*MATα ura3-52/ura3-52 lys2-801/+ his4-539/+ +/leu2-3,112 +/bik1-518 tub2-402/+*
L4400	*MAT***a**/*MATα ura3-52/ura3-52 leu2-3,112/leu2-3,112 his4-539/+ tub3::URA3/+ +/bik1-518*
L4401	*MAT***a**/*MATα ura3-52/ura3-52 his3Δ200/his3Δ200 leu2-3,112/+ +/lys2-801 cin1::HIS3/+ +/bik1-518*
L4402	*MAT***a**/*MATα ura3-52/ura3-52 leu2-3,112/leu2-3,112 his3Δ200/+ cin2::LEU2/+ +/bik1-518*
L4403	MAT**a**/*MATα ura3-52/ura3-52 leu2-3,112/leu2-3,112 his3Δ200/+ cin4::URA3/+ +/bik1-518*
S/B503	*MAT***a**/*MATα his1/+ trp1Δ1/trp1Δ1 ura3/+ leu2-3,112/+ cyh2/+ can1/+*
S/B 506	*MAT***a**/*MATα bik1-1::TRP1/bik1-1::TRP1 his1/+ trp1Δ1/ trp1Δ1 ura3/+ leu2-3,112/+ cyh2/+ can1/+* (isogenic with S/B 503)
S/B 551	L4320 transformed with pVB20
S/B 644	L4320 transformed with pRS314
VBY77	*MAT***a**/*MATα ura3-52/ura3-52 leu2-3,112/leu2-3,112 bik1-518/bik1-518* {pDAD2}
VBY79	*MAT***a**/*MATα ura3-52/ura3-52 leu2-3,112/leu2-3,112 bik1-518/bik1-518* {pVB20}
VBY82	*MAT***a**/*MATα ura3-52/ura3-52 leu2-3,112/leu2-3,112 bik1-518/bik1-518* {pVB24}
JY195	*MAT***a** *ura3-52 trp1Δ1 lys2-801 cyh2 bik1-518* [rho°] (J. Trueheart)

Braces indicate that the strain harbors the autonomously replicating plasmid whose name is contained within the backets. Brackets refer to the mitochondrial genotype.
:: indicates integration of the gene indicated after the symbol at the locus immediately preceding the symbol.
References for *tub* and *cin* alleles are: *tub1-1* (Stearns and Botstein, 1988); *tub2-104* and *tub2-105* (Thomas, 1985); *tub2-401*, *tub2-402*, *tub2-403*, *tub2-404*, *tub2-405* (Huffaker et al., 1988); *tub3* (Schatz et al., 1986b); *cin1::HIS3*, *cin2::LEU2*, and *cin4::URA3* (Stearns et al., 1990; Hoyt et al., 1990). All strains are from this work except where indicated.

Preparation of Antibody to the BIK1 Gene Product

The *E. coli* strain TG1 harboring pVB19 produced a fusion protein containing the first 324 amino acids of the TrpE protein, 10 amino acids of the polylinker, and 240 amino acids of BIK1. *trpE* expression was induced with indolacrylic acid (Koerner et al., 1990). An extract prepared from cells (8 ml total) lysed directly in Laemmli (1970) sample buffer was boiled, sonicated, and electrophoresed through a preparative 10% SDS-polyacrylamide gel. The gel was stained with 1% Coomassie blue in water for 15 min and then destained with several changes of water. The band corresponding to the fusion protein, ~68 kD in size, was excised from the gel and the fusion protein was electroeluted from the gel. Rabbits were injected intraperitoneally with 50 μg of the fusion protein mixed with an equal volume of Freund's adjuvant (Sigma Chemical Co.). Three and five weeks later rabbits were boosted with the same amount of fusion protein in an equal volume of Freund's incomplete adjuvant (Sigma Chemical Co.). 8 d after the last boost, blood was taken from the marginal ear vein by venipuncture.

Crude serum was adsorbed with cells containing a disruption of *BIK1*. 500 ml of log phase S/B 506 cells were pelleted and resuspended in 250 ml of 3.7% formaldehyde in 0.1 M KPO_4, pH 6.5. Cells were fixed for 12–16 h at room temperature, washed three times with PBS (137 mM NaCl, 3 mM KCl, 28 mM Na_2HPO_4, 1.5 mM KH_2PO_4, pH 7.3) and then once with PBS containing 1.2 M sorbitol. Cells were pelleted and resuspended in 25 ml lyticase buffer (1.2 M sorbitol, 25 mM KPO_4, pH 7.5, 2 mM $MgCl_2$, 2 mM DTT). Lyticase (Enzogenetics, Corvallis, OR) was added to a final concentration of 0.1 mg/ml and cells were digested at 30°C for 30 min with gentle shaking. Cells were washed three times with PBS, 1.2 M sorbitol containing protease inhibitors (PI; Sigma Chemical Co.): 5 μg/ml each of leupeptin, pepstatin, antipain, aprotinin; 1 μg/ml chymostatin; 1 mM each ε-aminocaproic acid and *p*-amino benzamidine; 0.25 mM PMSF. Cells were incubated in PBS containing 3% BSA and PI (PBS/BSA/PI) at 30°C for 30 min. Triton-X-100 was added to 0.1% and cells were incubated for 5 min at room temperature. Cells were washed with PBS/BSA/PI and then resuspended in 10 ml of PBS/BSA/PI plus 0.5% sodium azide to which 0.5 ml of crude serum was added. The cell suspension and crude serum was incubated at 4°C for 12–16 h with gentle shaking. Cells were pelleted and the supernatant was frozen in liquid nitrogen and stored at −70°C until further use.

Synchronization of Cells

Cells were grown overnight to saturation, diluted into fresh medium, and grown to a density of 10^7 cells/ml. Cells lacking plasmids or containing pVB20 or pRS314 were grown in SC medium or SC medium with uracil or tryptophan omitted for plasmid maintenance (growth medium). Cells were harvested by filtration on nitrocellulose filters (0.45 μm pore size; Nal-

gene Co., Rochester, NY) and resuspended in the same medium, adjusted to pH 4.0, to which α-factor was added to 5 μM. Cells were incubated at 30°C for 2 h at which time >90% of the cells were unbudded. Cells were harvested by filtration on nitrocellulose filters, washed and resuspended in growth medium and incubated for various times at 14 or 30°C.

Measurement of Chromosome Loss and Mitotic Recombination

The assay for chromosome loss and mitotic recombination is based on that of Wood and Hartwell (1982). Five colonies of each strain grown at 30°C were inoculated individually into YPD medium at a density of 10^7 cells/ml. Cultures were split and incubated at 30°C for 90 min or at 14°C for 24 h. Aliquots of each culture were then washed twice with water, diluted, and plated on YPD to measure the number of viable cells/ml and on SD containing 60 μg/ml canavanine and 20 mg/ml histidine. Colonies that grew on SD plus canavanine and histidine were replica-plated to SD and SD plus histidine. The frequency of mitotic recombination in the *CENV-CAN1* interval equals the number of His^+can^R cells/total viable cells and the frequency of loss of chromosome V equals the number of His^-can^R cells/total cells.

Analysis of Karyogamy

Matings were performed by mixing together 10^8 cells of each parent grown to log phase in YPD. Mixtures were pelleted, resuspended in 0.5 ml of YPD, spread on small YPD plates (60 × 15 cm), and incubated for various periods of time at 30°C. Mating mixtures were analyzed by fluorescence microscopy as described in a preceding section. To measure the formation of cytoductants, dilutions of the mating mixtures were plated on complete medium containing 3% glycerol, 0.1% glucose, and 10 μg/ml cycloheximide. Diploid formation and total cell counts were determined by plating dilutions of the mating mixtures on SD plus uracil and YPD, respectively.

Overexpression of BIK1 from the GAL1 Promoter

Cells were grown to log phase in SC medium minus uracil containing 2% raffinose instead of glucose. Galactose was added to 2% and aliquots were removed at various times for Western blot analysis, for immunofluorescence, and to monitor cell density.

Preparation of Cell Extracts and Immunoblotting

Whole cell extracts from yeast were prepared by glass bead lysis directly in trichloroacetic acid (Ohashi et al., 1987). Samples were analyzed by electrophoresis on 10% SDS-polyacrylamide gels (Laemmli, 1970), which were blotted electrophoretically onto nitrocellulose filters. Filters were incubated for 30 min with shaking in blocking solution: PBS containing 0.5% Tween 20 (vol/vol), 0.5% sodium azide (wt/vol) and 5% nonfat dry milk (wt/vol). Filters were then transferred to fresh blocking solution containing anti-BIK1 antibody (diluted 1/200), 206.1 anti-β-tubulin antibody (diluted 1/5,000), or 345 anti-α-tubulin antibody (diluted 1/5,000) (kindly provided by Frank Solomon) and incubated for 2 h at room temperature. Filters were given three 10 min washes in PBS containing 0.5% Tween 20 (PBS/Tween). Filters were then transferred to blocking solution containing ^{125}I-protein A (1 mCi/ml, 30 mCi/mg; Amersham Chemical Co., Arlington Heights, IL) diluted 1/1,000, incubated for 2 h at room temperature, and washed three times 10 min in PBS/Tween. Autoradiography was performed at −70°C using Kodak X-AR film. Western blots were quantitated according to the method of Suissa (1983).

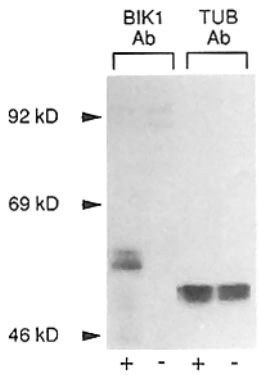

Figure 1. BIK1 and tubulin polypeptides in cell extracts of homozygous *BIK1/BIK1* and *bik1-1::TRP1/bik1-1::TRP1* diploids. Western blots of total cellular proteins isolated from homozygous diploids (*BIK1/BIK1*) (+) (L4320) and *bik1-1::TRP1/bik1-1::TRP1* (−) (L4324) were probed with anti-BIK1 (*BIK Ab*) and 206.1 and 345 antitubulin (*TUB Ab*) antibodies. BIK1 resolved as two species; often three species are apparent. The mobility of size markers is indicated on the left.

Computer Analysis of the BIK1 Amino Acid Sequence

Secondary structure analysis of BIK1 was performed using the Garnier et al., (1978) and Chou and Fasman (1978) algorithms. The National Biomedical Research Foundation Protein Sequence Database was searched with the entire BIK1 sequence using FASTA (Pearson and Lipman, 1988) and with the sequence $CX_2CX_3GHX_4C$ using MATCH (George et al., 1986). The sequence of BIK1 was compared directly to that of tau using FASTA (Pearson and Lipman, 1988). The statistical significance of sequence homologies was determined using IALIGN, an interactive version of the National Biomedical Research Foundation Align program (Dayhoff et al., 1983).

Results

Colocalization of BIK1 with Tubulin

Subcellular immunolocalization of the *BIK1* gene product was determined using antibodies raised against a TrpE-BIK1 fusion protein. The anti-BIK1 antibodies react with polypeptides 57–60 kD in size, which are present in extracts of wild-type cells but absent in extracts of *bik1-1::TRP1* strains containing a disruption of the *BIK1* gene. The BIK1 polypeptides often resolve as multiple species on Western blots and are distinguishable from the α- and β-tubulin polypeptides, 50–53 kD in size, which are present in extracts of both *BIK1* and *bik1-1::TRP1* strains (Fig. 1). Multiple species of BIK1 found on Western blots may be the consequence of posttranslational modification or proteolysis.

In an unsynchronized culture of exponentially growing cells anti-BIK1 antibodies stain structures that resemble intranuclear microtubules in 10–20% of the cells at 30°C and 30% of the cells at 14°C (results not shown). Enhanced immunolocalization of BIK1 at 14°C could be the consequence of the greater stability of BIK1 at low temperature or the detection of transient stages of growth in which BIK1 antigen is accessible to antibody binding. Although staining of microtubule structures with anti-BIK1 antibodies is detectable in cells containing a single copy of the *BIK1* gene, staining is more evident in a strain containing *BIK1* on the multicopy plasmid, pVB20. The steady state levels of the BIK1 polypeptide are two- to threefold higher in a strain containing pVB20 than a strain containing a single chromosomal copy of *BIK1* (results not shown).

The failure to detect staining of microtubule structures in a majority of cells in an unsynchronized culture could be explained by the association of the BIK1 protein with tubulin only during specific stages of the cell cycle. Thus the cell cycle dependence of BIK1 staining was examined by synchronizing cells with α-factor to obtain a homogeneous population of cells arrested at G1 and subsequently releasing them from arrest by transfer to fresh medium without α-factor. After release from α-factor arrest, cells were grown at 14°C. The slow doubling time at 14°C (6 h) facilitated the examination of cells at discrete stages of the cell cycle. Samples taken from the culture at various times after α-factor release were stained with both the antitubulin and anti-BIK1 antibody.

Immediately after release from α-factor arrest (results not shown) and at 1 h after release (Fig. 2), the anti-BIK1 antibodies stained the cytoplasm of unbudded cells, whereas the

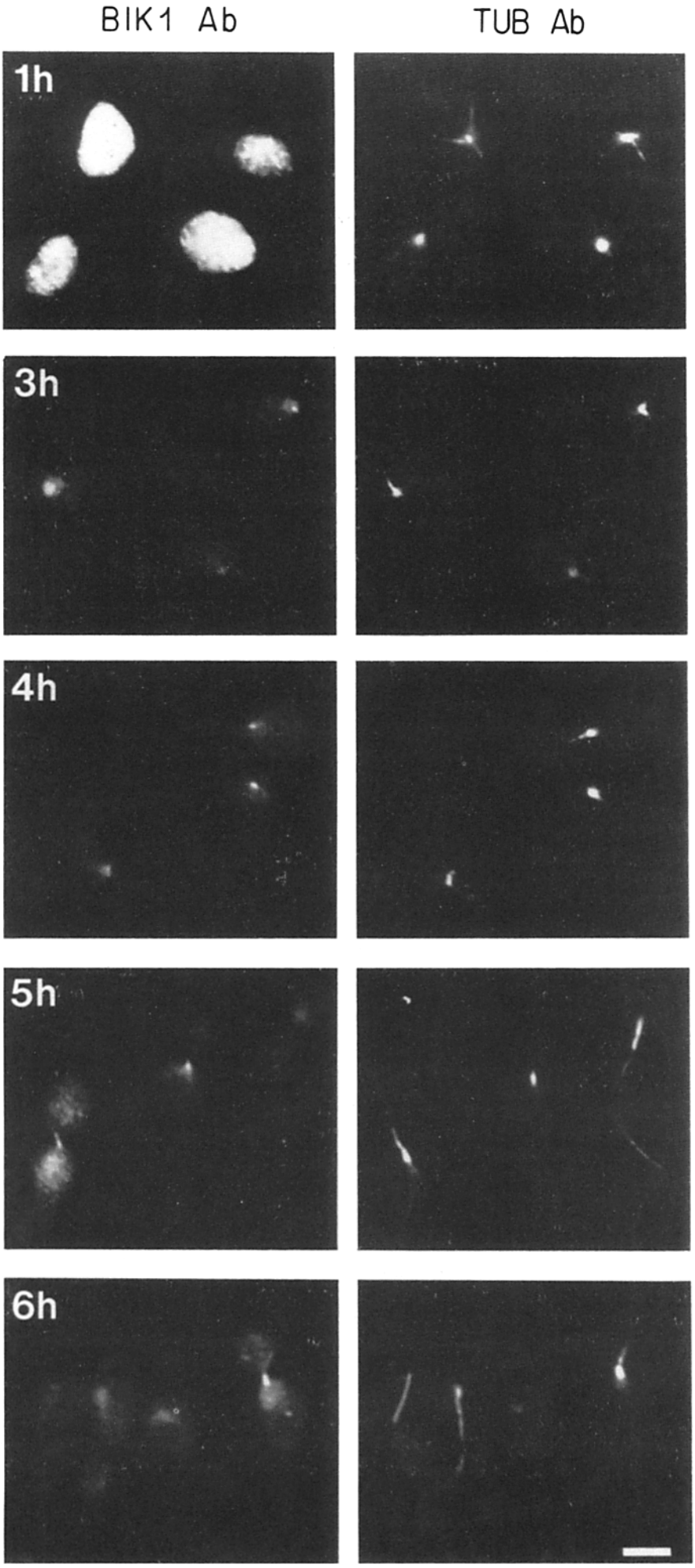

Figure 2. Fluorescence staining of synchronized wild-type cells with anti-BIK1 and antitubulin antibodies. Fluorescence images are of cells of strain S/B 551 double labeled with the anti-BIK1 (*BIK1 Ab*) (*left*) and the YOL1/34 antitubulin (*TUB Ab*) (*right*) antibodies, followed by staining with FITC- and Texas Red-conjugated secondary antibodies. Cells were grown for 1, 3, 4, 5, or 6 h after release from α-factor arrest at 14°C. Bar, 6 μm.

antitubulin antibody stained the spindle pole body and cytoplasmic microtubules. 3 and 4 h after release, BIK1 colocalized with tubulin to the spindle pole body in the nuclei of 60% of cells with nascent buds (Fig. 2). 5 and 6 h after release from growth arrest, BIK1 colocalized with tubulin in 40% of cells with short spindles and in twenty percent of cells with fully elongated spindles. The intensity of staining of spindle microtubules with anti-BIK1 antibodies was variable (Fig. 2). Cells containing a disruption of the *BIK1* gene failed to show any staining with the anti-BIK1 antibodies throughout the cell division cycle (results not shown).

Genetic Interaction between BIK1 and Genes Required for Microtubule Function in Yeast

The immunolocalization studies suggested a possible physical association between BIK1 and tubulin. The phenotype of double mutants between *bik1-518* and various mutations in the tubulin genes provided genetic evidence for this physical association. Double mutant meiotic segregants were obtained by crossing a *bik1-518* strain with strains containing mutations in *TUB1*, *TUB2*, or *TUB3*. The double mutants were tested for their growth at permissive and restrictive temperatures and sensitivity to the drug benomyl, a member of the benzimidazole class of compounds, which cause microtubule depolymerization in vivo (Jacobs et al., 1988) and in vitro (Kilmartin, 1981) and a failure of microtubule-mediated events in vivo (Quinlan et al., 1980; Delgado and Conde, 1984; Jacobs et al., 1988).

The growth of the double mutants was assessed in two ways: (*a*) by scoring directly the growth of the double-mutant ascospores and (*b*) by determining survival of vegetative double-mutant cells upon loss of a plasmid containing either a functional *BIK1* or *TUB* gene. The ascospore germination test was complicated by growth-enhancing suppressors that arose during germination or growth of the spore clones. These occurred frequently and made the primary phenotypes of the double mutants difficult to determine. The plasmid segregation test was more easily interpreted because it was possible to produce a homogeneous population of vegetative cells of the same genotype whose phenotype, upon loss of the plasmid, could be assessed. In the plasmid segregation test, we found that the majority of the double mutants did not grow at 30°C or had a slow growth phenotype (Table III). Epistasis relationships were examined in the viable double mutant strains. The *bik1-518 tub2-104* and *bik1-518 tub2-402* mutants exhibited benomyl sensitivity equivalent to the *bik1-518* strain, indicating that *bik1-518* is epistatic to *tub2-104* and *tub2-402*, which as single mutants confer resistance to high levels of benomyl (Thomas, 1985; Huffaker et al., 1988). A possible explanation for the epistasis relationships is that the *bik1-518* mutation alters the structural properties of tubulin such that tubulin binds benomyl in the double mutants, but not in the *tub2-104* and *tub2-402* single mutants.

A *bik1-518* strain was also crossed to strains carrying *cin1*, *cin2*, or *cin4* mutations, which cause chromosome instability (Hoyt et al., 1989) and, like *bik1-518*, cause cold sensitivity, hypersensitivity to benomyl, and lethality in combination with the *tub1-1* allele (Stearns et al., 1990; Hoyt et al., 1990). The double mutants exhibited a slow growth phenotype at 30°C (Table III), a permissive temperature for growth of the single mutants, and also grew more slowly than the single mutants at 14°C. Both *bik1-518 cin1::HIS3* and *bik1-518 cin2::LEU2* strains exhibited variable levels of sensitivity to benomyl, suggesting that suppressors arise frequently in the double mutants. The *bik1-518 cin4::URA3* double mutant exhibited benomyl sensitivity equivalent to that of the *cin4::URA3* parent, indicating *cin4::URA3* is epistatic to *bik1-518*.

Table III. Growth of Double Mutants

Genotype	Ascospore*	Vegetative cell‡
Wild type	++++	++++
Single mutant§	++++	++++
bik1-518 tub1-1 (L4392)	−	−
bik1-518 tub2-105 (L4393)	−	−
bik1-518 tub2-401 (L4394)	+	−
bik1-518 tub2-403 (L4395)	+	−
bik1-518 tub2-404 (L4396)	+	−
bik1-518 tub2-405 (L4397)	+	+
bik1-518 tub2-104 (L4398)	+	+
bik1-518 tub2-402 (L4399)	++	++
bik1-518 tub3 (L4400)	+	+++
bik1-518 cin1::HIS3 (L4401)	+	+
bik1-518 cin2::LEU2 (L4402)	+	+
bik1-518 cin4::URA3 (L4403)	++	ND

* Ascospore segregants were obtained by sporulating the diploid strains L4392-L4403, indicated in parentheses, and were grown at 30°C. Minus indicates no growth. The plusses indicate a range of growth from very slow growth (+) to moderately slow growth (+++) compared with wild-type and single mutants.

‡ Vegetative cells containing plasmids were obtained by sporulating diploid strains transformed with various plasmids before sporulation: L4392-L4399, L4402, and L4403 were transformed with pVB20; L4400 was transformed with pRB327; L4401 was transformed with pRB1171. Minues indicates inability to lose pVB20, pRB327, or pRB1171 spontaneously or on medium containing 5-fluoro-orotic acid (Boeke et al., 1984) which selects for loss of the *URA3*-containing plasmids pVB20 and pRB1171. The plusses indicate a range of growth from very slow growth (+) to moderately slow growth (+++) compared with growth of the wild type and single mutants after plasmid loss.

§ Refers to *bik1-518*, *tub1-1*, *tub2* (any of the alleles listed), *cin1::HIS3*, *cin2::LEU2*, or *cin4::URA3* none of which has a discernible growth defect at 30°C.

BIK1 Is Required for Normal Microtubule Structures

If BIK1 is a structural component of microtubules, as the immunolocalization and genetic studies suggest, absence of BIK1 should cause altered microtubule assembly. To investigate this possibility, microtubule structures in *BIK1* and *bik1-1::TRP1* cells were compared. Cells were synchronized with α-factor and then grown at 14°C, at which temperature the doubling time of *bik1-1::TRP1* cells is approximately twice that of wild type cells (results not shown). In unbudded *BIK1* cells, cytoplasmic microtubules emanate from a single spindle pole body (Fig. 3 *A*). In *BIK1* cells with nascent buds, a subset of microtubules appears to point toward the site of

Figure 3. Microtubule structures in synchronized *BIK1/BIK1* and *bik1-1::TRP1/bik1-1::TRP1* cells. Homozygous *BIK1/BIK1* (L4320) and *bik1-1::TRP1/bik1-1::TRP1* (L4324) diploids were grown for 1, 3, 4, 5, and 6 h (*A–E*) at 14°C after release from α-factor arrest. The far left and far right columns show the Nomarski images of cell morphology and DAPI fluorescence of cellular DNA. The center columns show staining of microtubule structures with 206.1 antitubulin antibody (TUBULIN) and FITC-conjugated secondary antibody. Bar, 7.5 μm.

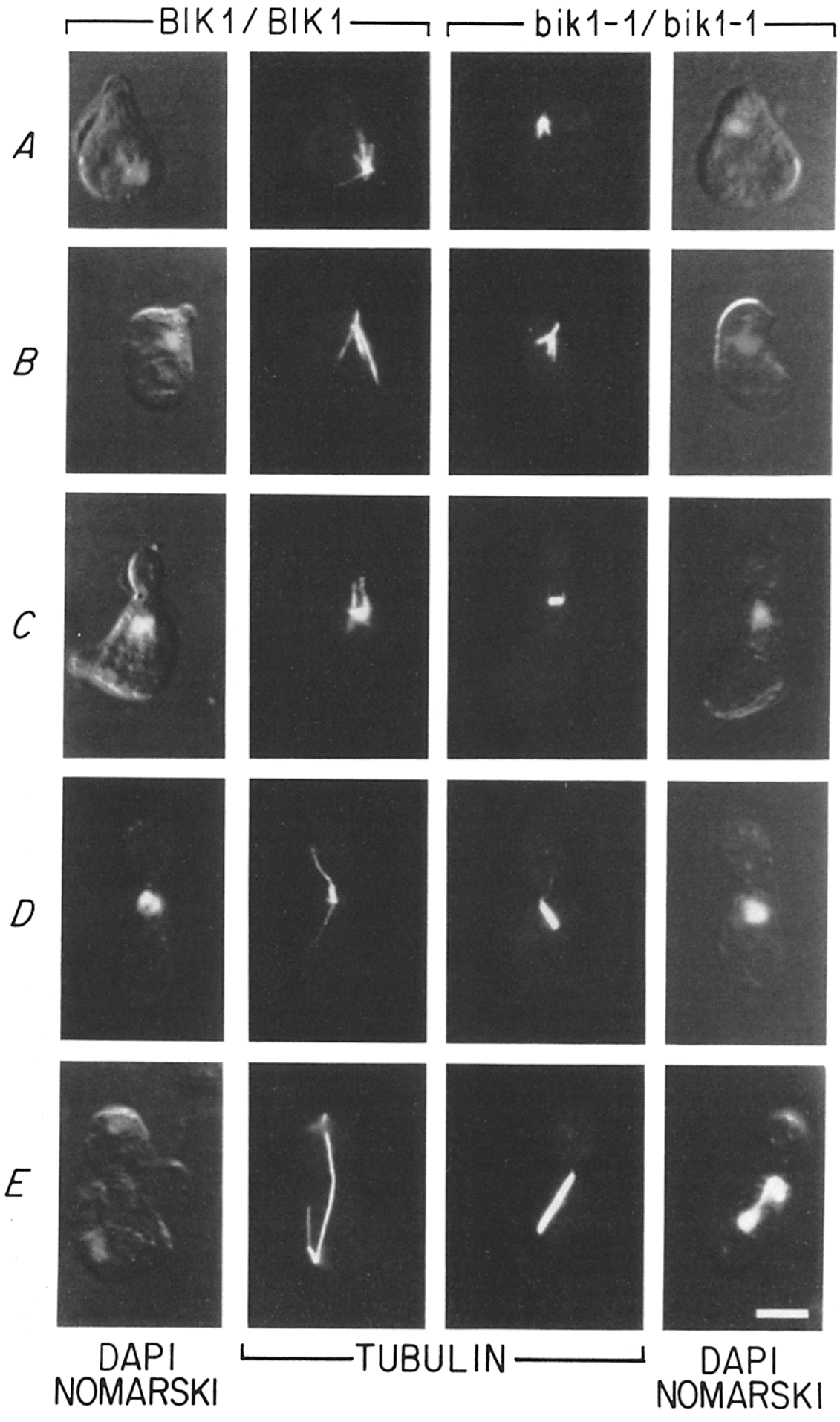
BIK1/BIK1
bik1-1/bik1-1
A
B
C
D
E
DAPI
NOMARSKI
TUBULIN
DAPI
NOMARSKI

bud emergence (Fig. 3 *B*). Cytoplasmic microtubules in *bik1-1::TRP1* cells at the same stages of division are absent or abnormally short (Fig. 3, *A* and *B*). During bud formation in a *BIK1* cell, the nucleus move to the neck; the spindle pole body duplicates and moves to opposite poles, forming a short spindle. In small-budded BIK1 cells, the cytoplasmic microtubules extend from one or both spindle pole bodies towards the neck of the bud (Fig. 3 *C*). Cells with both sets of microtubules pointing toward the bud are routinely observed in synchronized populations of cells grown at 14°C but rarely in unsynchronized cells, suggesting this may be a transient stage of cell division. As the bud grows, the spindle lengthens near the neck of the bud and cytoplasmic microtubules extend from one spindle pole body into the mother cell and from the other spindle pole body through the neck into the daughter cell (Fig. 3 *D*). In *bik1-1::TRP1* cells with buds, the cytoplasmic microtubules are usually absent; when they are visible, they are abnormally short (Fig. 3, *C* and *D*). During anaphase the spindle in *BIK1* cells elongates until it extends from one pole in the mother cell to the opposite pole in the daughter cell; the cytoplasmic microtubules splay out from the spindle pole bodies which appear to abut the cell perimeter. *bik1-1::TRP1* cells are quite different: the anaphase spindle is always shorter than that in *BIK1* cells. Moreover spindle elongation often occurs within the confines of one member of a budded pair (mother or daughter), a situation never observed in wild type cells. In those *bik1-1::TRP1* cells were the spindle traverses the neck, it rarely (as contrasted with wild-type cells) extends the full length of the mother and daughter cells. As in earlier stages of division, cytoplasmic microtubules in *bik1-1::TRP1* cells are absent or abnormally short (Fig. 3 *E*).

BIK1 Is Required for Proper Nuclear Segregation during Mitosis

bik1-1::TRP1 cells show aberrant nuclear segregation, consistent with mislocalization of the spindle during mitosis. At 30°C, 5–10% of the cells are anucleate or multinucleate and at 14°C, the fraction of multinucleate and anucleate cells increases to 10–20% of the total, consistent with the slow growth of *bik1-1::TRP1* strains at low temperature. In *BIK1* cultures grown at 30 or 14°C, 1% of the cells are multinucleate or anucleate.

The basis of the defect in nuclear segregation during mitosis in *bik1-1::TRP1* cells was determined by monitoring nuclear position in diploid cells (*BIK1/BIK1* and *bik1-1::TRP1/bik1-1::TRP1*) synchronized with α-factor. Cells were monitored for two cell-division cycles after release from α-factor arrest. The rates of bud formation and release were equivalent during this time period for *BIK1/BIK1* and *bik1-1::TRP1-1/bik1-1::TRP1-1* cultures grown at 30 or 14°C (results not shown). Prior to anaphase, nuclear DNA is located either in the mother cell or spanning the neck between mother and daughter cells in a majority of *BIK1/BIK1* and *bik1-1::TRP1-1/bik1-1::TRP1-1* cells grown at 30 and 14°C. A larger percentage of *BIK1/BIK1* cells have nuclear DNA spanning the neck compared with *bik1-1::TRP1-1/bik1-1::TRP1-1* cells grown at either 30 or 14°C (Table IV). During anaphase, nuclear DNA segregates properly to mother and daughter cells in virtually all of the *BIK1/BIK1* cells grown at 30 or 14°C. In contrast, nuclear DNA segregation occurs within the confines of the mother cell in a significant fraction of *bik1-1::TRP1-1/bik1-1::TRP1-1* cells (10–34%) grown at 30°C. At 14°C, a percentage of *bik1-1::TRP1/bik1-1::TRP1* cells in which anaphase occurs strictly within the mother cell ranges from 12 to 26% during the first cell division cycle and increases to 43–46% during the second cell division cycle (Table V). The percentage of binucleate *bik1-1::TRP1/bik1-1::TRP1* cells decreases as cells progress through the cell cycle (Table V), suggesting that one of the two nuclei can migrate through the neck into the bud before cytokinesis.

Table IV. Position of Nuclear DNA before Anaphase

	BIK1/BIK1				*bik1-1::TRP1/bik1-1::TRP1*			
30°C		Nuclear position§				Nuclear position§		
Cell division cycle*	% Budded cells‡	M	N	B	% Budded cells‡	M	N	B
1 (1)	81	80	17	3	89	91	8	1
1 (1.2)	84	74	21	5	93	94	4	2
2 (2.5)	72	68	29	4	88	96	3	1
2 (2.7)	69	63	30	7	67	96	3	1
14°C								
1 (3)	78	73	23	4	91	95	4	1
1 (4)	92	61	30	9	93	93	5	2
2 (7)	75	84	12	4	73	97	2	1
2 (8)	59	85	11	4	57	97	2	1

* The number of cell division cycles after release from α-factor arrest. Indicated in parentheses is the time in hours after release from α-factor arrest.
‡ The percentage of budded cells at specific times after release from α-factor arrest.
§ The percentage of cells with nuclear DNA located in the mother cell (*M*), spanning the neck (*N*), or in the bud (*B*) as determined by DAPI staining. Percentages are based on the examination of 200–300 cells for each time point. The strains examined were S/B644 (*BIK1/BIK1*) and L4324 (*bik1-1::TRP1/bik1-1::TRP1*).

BIK1 Is Required for Chromosome Stability

The requirement of BIK1 for spindle function was examined by assaying the stability of chromosome V in isogenic *BIK1/BIK1* and *bik1-1::TRP1/bik1-1::TRP1* diploids grown at

Table V. Position of Nuclear DNA during Anaphase

	BIK1/BIK1				*bik1-1::TRP1/bik1-1::TRP1*			
30°C		Nuclear position§				Nuclear position§		
Cell division cycle*	% Budded cells‡	1M1B	2M	2B	% Budded cells‡	1M1B	2M	2B
1 (1.2)	81	100	0	0	93	66	34	0
1 (1.3)	84	99	1	0	92	87	13	0
2 (2.5)	72	100	0	0	88	89	11	0
2 (2.7)	69	100	0	0	67	90	10	0
14°C								
1 (3)	78	100	0	0	91	73	26	1
1 (4)	92	100	0	0	93	87	12	1
2 (7)	75	99	1	0	73	51	48	1
2 (8)	59	100	0	0	57	57	43	0

*‡ As in Table IV.
§ The percentage of cells in which nuclear DNA segregated to mother and bud (1M1B), segregated within the mother cell (*2M*), or segregated within the bud (*2B*), as monitored by DAPI staining. Percentages are based on the examination of 200–300 cells for each time point. The strains used were the same as those described in Table IV.

30 or 14°C. Loss of chromosome V was measured in cells from five independent colonies of each strain. As Table VI indicates, the frequency of chromosome loss in the *bik1-1::TRP1/bik1-1::TRP1* diploids was on average 10-fold greater than in wild-type diploids grown at 30 or 14°C. The elevation of chromosome loss in *bik1-1::TRP1/bik1-1::TRP1* diploids could be due to nondisjunction or to defects in DNA metabolism. To distinguish between these two possibilities, we used the frequency of mitotic recombination as a measure of defects in DNA metabolism. We found that the frequency of mitotic recombination in the *bik1-1::TRP1/bik1-1::TRP1* strain was equivalent to that in the *BIK1/BIK1* strain, when grown either at 30 or 14°C, suggesting that the former does not have enhanced DNA damage.

Overexpression of the BIK1 Product Causes Cell Division Cycle Arrest

The *BIK1* promoter was replaced with the inducible *GAL1* promoter to assess the effect of overexpression of *BIK1* on cell growth. When a plasmid containing the *GAL1-BIK1* fusion was introduced into a *bik1-518/bik1-518* strain, the strain failed to grow on medium containing galactose but was able to grow on medium containing glucose. The effect of *BIK1* overexpression was also examined by adding galactose to the *GAL1-BIK1* strain growing in liquid medium containing raffinose, which does not induce or repress expression from the *GAL1* promoter. 9 h after addition of galactose to the medium, strains containing the *GAL1-BIK1* fusion plasmid had achieved less than one cell doubling before stopping proliferation, whereas strains containing control plasmids doubled approximately four times and continued to increase in cell number (Fig. 4 *A*). Western analysis demonstrated that in VBY82, the strain containing the *GAL-BIK1* fusion plasmid, expression of *BIK1* was indeed regulated by galactose (Fig. 4 *B*). The BIK1 polypeptide did not accumulate in VBY82 cells prior to the addition of galactose to the medium. Two hours after addition of galactose to the medium, VBY82 had fourfold higher levels of the BIK1 polypeptide and eightfold higher levels by 9 h, compared with strain VBY79, which contained a plasmid with the *BIK1* gene expressed from its own promoter.

4 h after the addition of galactose to the medium, >70% of the *bik1-518/bik1-518* cells with the *GAL1-BIK1* fusion plasmid had a distinctive cell division cycle morphology: they arrested division as large-budded cells containing a single nucleus located in or adjacent to the neck separating the mother cell from the bud. Before addition of galactose to the medium, a majority of large budded cells stained with antitubulin antibody had microtubule structures characteristic of a *bik1-518/bik1-518* strain, i.e., a short anaphase spindle devoid of detectable cytoplasmic microtubules emanating from the spindle pole bodies. 2 h after the addition of galactose to the medium, a significant fraction of large budded *bik1-518/bik1-518 GAL-BIK1* cells had long cytoplasmic microtubules. We were unable to distinguish whether the cytoplasmic microtubules extended from a single spindle pole body or from duplicated, unseparated spindle pole bodies (Fig. 5). At later times after the addition of galactose to the

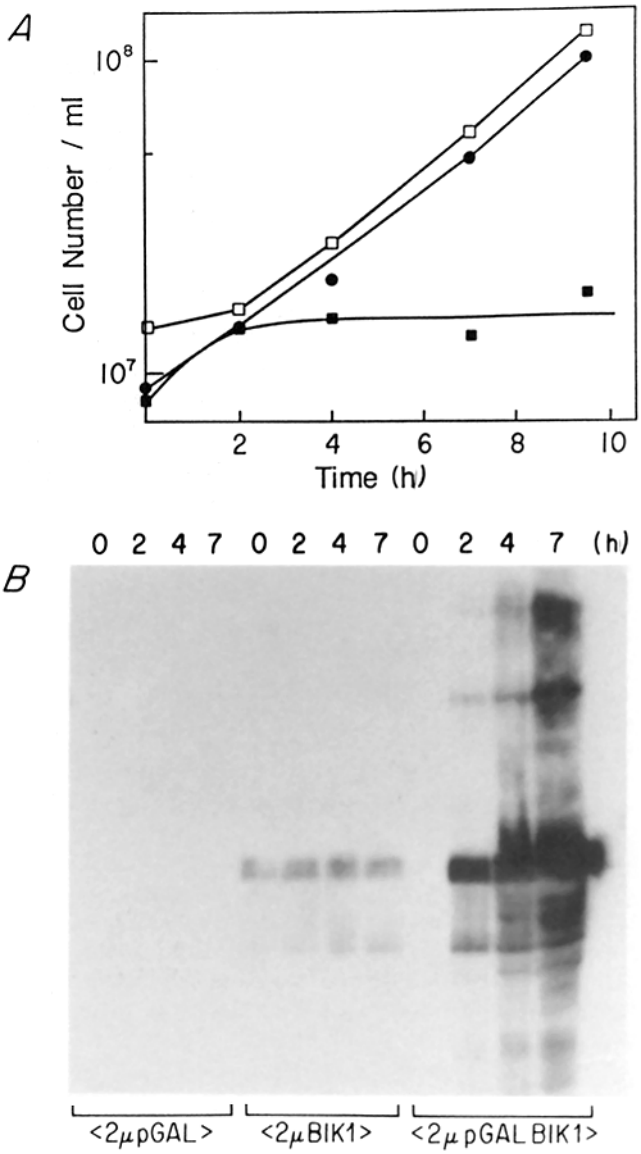

Figure 4. Division arrest of cells expressing *BIK1* from the *GAL1* promoter. (*a*) Cell densities of *bik1-518/bik1-518* transformants VBY77, VBY79, and VBY82 containing pDAD2 (*GAL1* promoter plasmid; ●), pVB20 (*BIK1* plasmid; □), and pVB24 (*GAL-BIK1* fusion plasmid; ■), respectively, are plotted versus time after addition of galactose to cell cultures pregrown in medium containing raffinose. (*b*) Western blots of protein extracts prepared from VBY77 (*2μ pGAL*), VBY79 (*2 μ BIK1*), and VBY82 (*2 μ pGAL BIK1*) grown for various times indicated in hours (*h*) after addition of galactose to the medium were probed with anti-BIK1 antibody and ^{125}I-protein A.

Table VI. Chromosome Loss and Mitotic Recombination

	Frequency (× 10^{-5})			
	Chromosome loss		Mitotic recombination	
Diploid strain	14°	30°	14°	30°
BIK1/BIK	5.9	4.4	18.4	16.5
bik1-1::TRP1/bik1-1::TRP1	60.5	45.8	23.0	14.5

Numbers listed are averages of five independent assays. The strains used were S/B503 (*BIK1/BIK1*) and S/B506 (*bik1-1::TRP1/bik1-1::TRP1*).

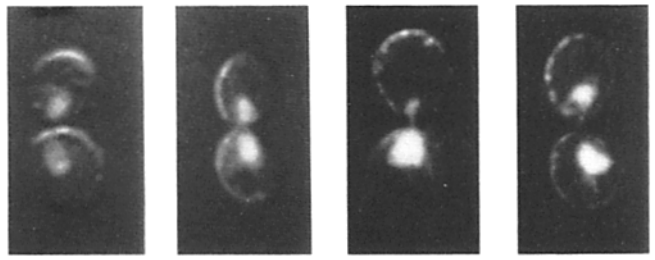

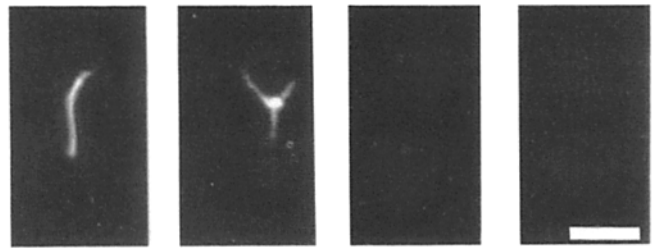

H				
0	99.0	0.5	0.5	0.0
2	68.0	27.0	5.0	0.0
4	29.0	33.0	21.0	17.0
8	5.5	42.5	17.0	35.0

Figure 5. Microtubule structures in cells expressing *BIK1* from the *GAL1* promoter. A *bik1-518* strain (VBY82) containing pVB24 (*GAL-BIK1* fusion plasmid) was grown for 0, 2, 4, or 8 h after addition of galactose to raffinose medium. Cells were stained with DAPI, YOL1/34 antitubulin antibody, and Texas Red–conjugated secondary antibody. The DAPI and Nomarski images (*DAPI/NOM*) are corresponding tubulin staining (*TUB*) are shown for representative cells. The numbers are the percentages of cells at each time point with microtubule structures comparable to those shown in the photographs above each column. 200 cells were examined at each time point. Bar, 6 μm.

medium, 40–50% of the large budded cells contained residual or no microtubule structures (Fig. 5). These data suggest that overexpression of the *BIK1* gene initially blocks spindle formation while promoting the formation of cytoplasmic microtubules, and then subsequently causes the loss of microtubule structures.

BIK1 Is Required for Nuclear Fusion

Cytological observations show that >90% of *bik1* × *bik1* zygotes have unfused nuclei even though the frequency of zygote formation is comparable to that in wild-type crosses. Genetic evidence for the failure of nuclear fusion in *bik1* × *bik1* crosses is demonstrated by the high frequency of cytoduction in such crosses. Cytoductants are haploid exconjugants resulting from cell fusion and cytoplasmic mixing without nuclear fusion. The results in Table VII indicate that the frequency of diploid formation is 10-fold lower and the ratio of cytoductants-to-diploids is 10,000-fold greater in matings between two *bik1-518* strains compared to that in matings in which one or both of the parents is *BIK1*. The high ratio of cytoductants to diploids in *bik1-518* × *bik1-518* matings indicates that diploid formation is blocked after cell fusion and before nuclear fusion. Nuclear fusion is impaired to a similar degree by the *kar1-1* mutation, which unilaterally blocks nuclear fusion (Rose and Fink, 1987).

We examined the microtubules in zygotes by indirect immunofluorescence using an antibody against tubulin. Immediately after cell fusion and prior to nuclear fusion, the spindle pole bodies are juxtaposed in a majority of zygotes regardless of the presence or absence of BIK1 product. Subsequent fusion of the spindle pole bodies is observed in a majority of zygotes containing the BIK1 product, but is rarely seen in zygotes lacking it. *bik1-1* × *bik1-1* zygotes with unfused spindle pole bodies, the nuclei have separated (Fig. 6).

Cytoplasmic microtubules in *bik1* × *bik1* zygotes are absent or abnormally short. The relatively small size of the cytoplasmic microtubules in a wild type cell makes the assessment of this phenotype difficult. Therefore, the effects of the *bik1-518* mutation in *kar1-1* cells were examined. *kar1-1* cells produce abnormally long cytoplasmic microtubules (Rose and Fink, 1987), making the distinction between the presence and absence of microtubules much clearer. We observed in a cross of *bik1-518 kar1-1* × *bik1-518* than neither nucleus has discernable cytoplasmic microtubules (Fig. 7). This result clearly implicates BIK1 in the formation or stability of cytoplasmic microtubules.

Table VII. Diploid Frequency and Cytoductant to Diploid Ratio in Crosses of bik1-518 and kar1-1 Mutants

Parent *MATa* [rho°] Cyh^r	Parent *MATα* [rho$^+$] Cyh^s	Diploid/ Total*	Cytoductant/ Diploid‡
BIK1	*BIK1*	0.5	0.0004
BIK1	*bik1-518*	0.6	0.002
bik1-518	*BIK1*	0.32	0.001
bik1-518	*bik1-518*	0.02	3.2
BIK1kar1-1	*BIK1KAR1*	0.05	3.7

* Prototrophic colonies/total colonies
‡ Cyh^r [p$^+$] colonies/prototrophic colonies
Strains used were L2964 (*MATaBIK1*), L2736 (*MATαBIK1*), *JY195* (*MATabik1-518*), L2751 (*MATαbik1-518*), L2965 (*MATakar1-1*).

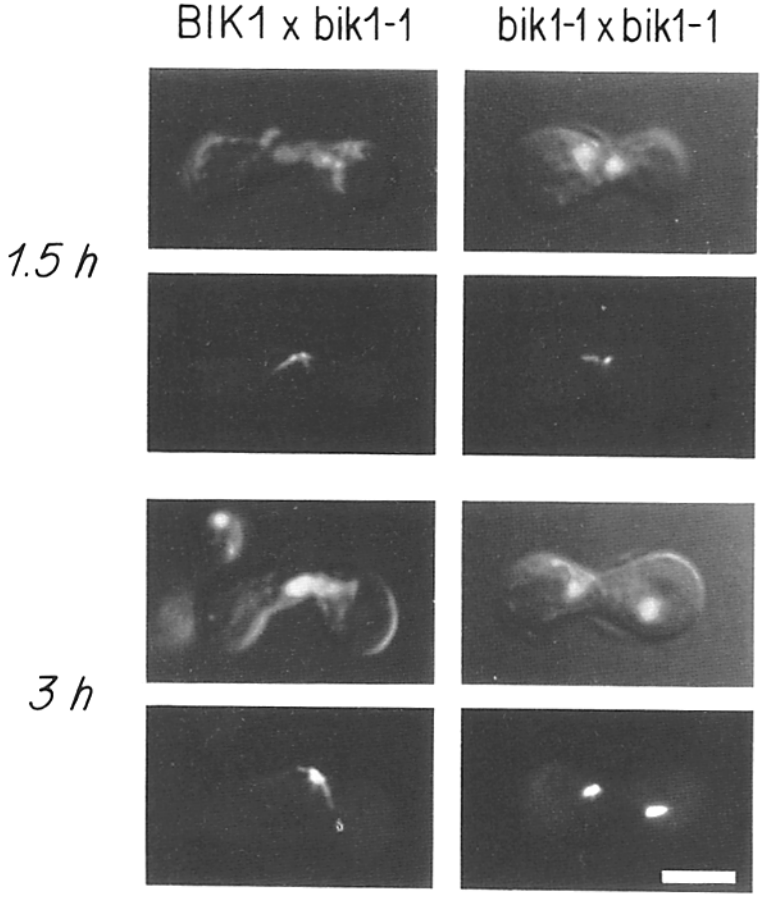

Figure 6. DAPI and antitubulin staining of zygotes. Shown are *BIK1* × *bik1-1::TRP1* (L3758 × L3763) and *bik1-1::TRP1* × *bik1-1::TRP1* (L3762 × L3763) zygotes present at 1.5 or 3 h after mixing *MAT***a** and *MAT*α parents. (*Top*) DAPI/Nomarski images at each time point, (*bottom*) the same zygotes stained with 206.1 antitubulin antibody and FITC-conjugated secondary antibody. Bar, 6 μm.

Sequence Homologies within the Putative Structural Domains of BIK1

The amino acid sequence of BIK1 deduced from the nucleotide sequence was determined previously (Trueheart et al., 1987). The Chou-Fasman and Garnier algorithms (Chou and Fasman, 1978; Garnier et al., 1978), used to predict protein secondary structure, suggest that BIK1 has three structural domains (Fig. 8). The amino-terminal region of 193 residues contains alternating regions predicted to form α-helices, β-sheets, β-turns, and random coils, which is characteristic of globular proteins. From amino acids 194 to 398 is a region predicted to be α-helical. The carboxy-terminal region, from amino acids 394 to 440, contains a high proportion of amino acids predicted to form β-turns.

A sequence at the amino terminus of BIK1, extending from amino acids 2 to 26, shows similarity to the mammalian microtubule-associated protein tau (Fig. 8). Within the tau sequence that shows similarity to BIK1 is an 18-amino acid motif that is repeated three times in tau (Lee et al., 1988). The region in tau containing these repeats and a homologous region in MAP2 are rich in basic amino acids and bind microtubules (Lewis et al., 1988; Lee et al., 1989; Lewis et al., 1989). Synthetic peptides corresponding to the acidic carboxy-terminal domain of tubulin bind both tau and MAP2 (Maccioni et al., 1988), suggesting that the basic regions in tau and MAP2 may interact electrostatically with the acidic domain of tubulin. The region in BIK1 which shows similarity to tau is basic; the entire region from amino acid 1 to 126 has a calculated pI of 11.3. In contrast, the region in BIK1 from amino acid 127 to 440 is acidic with a calculated PI of 4.9.

The carboxy terminus of BIK1, from amino acids 416 to 429, has the metal binding motif, C-X_2-C-X_4-H-X_4-C (X is

Figure 7. Cytoplasmic microtubules in Bik$^+$ and Bik$^-$ zygotes having a *kar1-1* parent. Shown are zygotes present four hours after mixing strains L2753 (*bik1-518 kar1-1*) and L2736 (*BIK1 KAR1*) or L2751 (*bik1-518 KAR1*); zygotes were stained with YOL1/34 antitubulin antibody and Texas Red–conjugated secondary antibody. Bar, 6 μm.

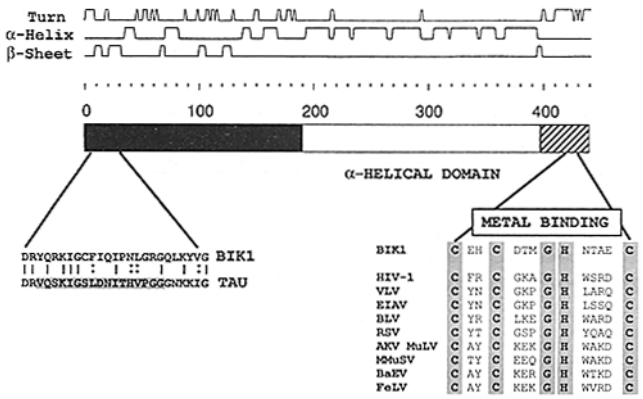

Figure 8. Sequence homologies within putative structural domains of BIK1. The Garnier secondary structure predictions (Garnier et al., 1978) are shown above a schematic diagram of the BIK1 polypeptide, which is divided into three putative domains. The scale indicates amino-acid position in the BIK1 polypeptide. In the amino-terminal domain (*solid black*) is a sequence that shows 40% identity to a region in tau. The alignment score, based on 1,000 randomized runs, is 6 SD from the mean. The solid bars designate amino acid identities and the colons designate similar amino acids. The sequence repeated three times in tau is shaded. The central region of BIK1 (*white*) appears to be α-helical and shows 26% identity with the rod domain of the myosin alpha heavy chain from rabbit cardiac muscle. The homology to myosin is dispersed throughout this region (results not shown). The alignment score based on 100 randomized runs is 5 SD from the mean. In the carboxy terminus of BIK1 (*hatched region*) is a metal binding motif (*shaded residues*) found in retroviral *gag*-encoded nucleocapsid proteins of which several are listed (taken from Berg, 1986).

any amino acid) found in retroviral *gag*-encoded nucleocapsid proteins (Berg, 1986; Green and Berg, 1989; South et al., 1989), the *Drosophila* copia element (Mount and Rubin, 1985), and cauliflower mosaic virus (Franck et al., 1980) (Fig. 8). This sequence is similar to "zinc finger" domains which bind nuclei acid (Miller et al., 1985; Brown et al., 1985).

The α-helical region of BIK1 shows similarity to the rod domains of several myosin heavy chains. BIK1 shows the greatest homology to the myosin α heavy chain from rabbit cardiac muscle (see legend to Fig. 8). Within the putative α-helical region of BIK1 are 27 heptad repeats characteristic of myosin and intermediate filament proteins. Hydrophobic residues are located preferentially at the first and fourth positions of the repeat while charged residues preferentially occupy the remaining positions of the repeat (McLachlan and Karn, 1983) (Fig. 9). Two regions (amino acids 292–301 and 358–363) contain helix disrupting proline residues and interrupt the heptad repeats. Proteins containing heptad repeats form coiled-coil structures: α-helices that coil around one another in a regular helical structure stabilized by interactions between hydrophobic residues on intertwined helices.

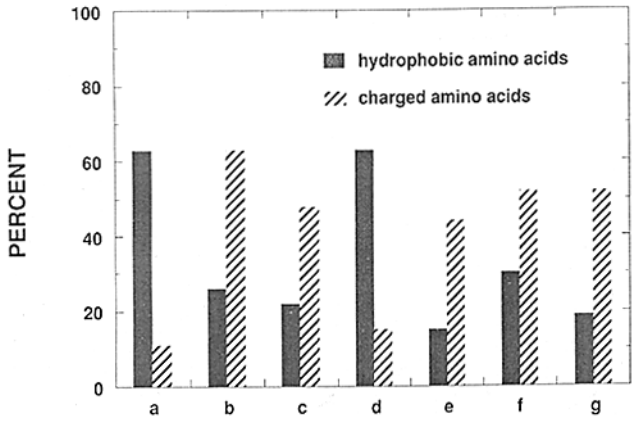

Figure 9. Heptad repeats in BIK1. The histograms show the percentage of hydrophobic and charged residues in the positions (*abcedfg*) of the 27 heptad repeats in the α-helical region of BIK1 extending from amino acid 194 to 398.

Discussion

The BIK1 protein of yeast displays properties expected of a structural component of the microtubule cytoskeleton. First of all, the BIK1 protein colocalizes with tubulin. In addition mutations in *BIK1* cause aberrant nuclear segregation during mitosis, chromosome instability, and blocked nuclear fusion. These defects in microtubule function correlate with altered microtubule morphologies. The most dramatic morphological defect in *bik1* cells is in the cytoplasmic microtubules, which are either absent or abnormally short. The location of the cytoplasmic microtubules in wild type cells and absence in nocodazole-treated cells and *tub2* mutants defective in nuclear migration (Jacobs et al., 1988; Huffaker et al., 1988) suggest they may be required to orient the spindle properly or to guide the nucleus into the bud. If so, defective cytoplasmic microtubules could give rise to the anucleate and multinucleate cells present in *bik1* cultures. Elevated levels of chromosome loss in the *bik1-1::TRP1* mutant are indicative of defective spindle function. The mitotic defects of *bik1* null mutants are not lethal. Proteins functionally redundant with BIK1 could account for the viability of *bik1* null mutants.

Mutations in *BIK1* also affect the cytoplasmic microtubules during zygote formation. The absence of cytoplasmic microtubules observed in *bik1* × *bik1* crosses may account for the absence of nuclear fusion in such matings. The cytoplasmic microtubules, which connect the spindle pole bodies on the haploid nuclei, are thought to pull the nuclei together (Byers and Goetsch, 1974, 1975; Meluh and Rose, 1990). One explanation for the failure of fusion in *bik1* crosses might be that the nuclei are unable to migrate toward each other early in zygote formation. Were this correct, we would have expected the nuclei of mating *bik1* cells to be located randomly in the zygotes. However, the nuclei and spindle pole bodies are appropriately juxtaposed early in zygote formation. The subsequent retreat of unfused haploid nuclei to midcell positions suggests that BIK1 is critical to a late step in migration that may be closely linked to nuclear fusion.

Overexpression of *BIK1* from the *GAL1* promoter has a profound effect on the microtubule cytoskeleton. Initially, overexpression of *BIK1* results in the production of large-budded cells which contain extralong cytoplasmic microtubules, but lack spindle microtubules. This phenotype contrasts with the absence of the cytoplasmic microtubules in the *bik1* mutant. Cells overexpressing *BIK1* accomplish a single doubling and then cease dividing. Arrest in cell divi-

sion coincides with the appearance of cells lacking nuclear and cytoplasmic microtubules. Disappearance of microtubule structures is also observed in strains over-expressing the *TUB2* gene from the *GAL1* promoter (Burke et al., 1989). These results are consistent with the notion that BIK1 and the tubulin subunits are required in the proper stoichiometry for the assembly or stability of microtubules.

Double labeling of synchronized cells by indirect immunofluorescence using anti-BIK1 and antitubulin antibodies indicates BIK1 colocalizes with tubulin. The pattern of staining with BIK1 antibodies changes as cells progress through the cell cycle. BIK1 antibodies stain the cytoplasm of unbudded cells. We have not ruled out the possibility that levels of the BIK1 antigen change during the cell cycle or that the cytoplasmic staining with the BIK1 antibodies obscures staining of nuclear structures. The cytoplasmic staining is most likely not a consequence of treatment with α-factor, because BIK1 antibodies stain the cytoplasm of unbudded cells which were not treated with α-factor (results not shown). Colocalization of BIK1 with tubulin was observed during the initial stages of bud formation. Anti-BIK1 antibodies stained the spindle pole body most prominently, whereas staining of the mitotic spindle was variable. Several factors may be responsible for the variability of staining of the mitotic spindle: (*a*) BIK1 may dissociate from the spindle; (*b*) the BIK1 antigen may be unstable in cells during spindle formation; (*c*) the anti-BIK1 epitope may not be as accessible to binding antibody at this stage of division. We were unable to detect staining of the cytoplasmic microtubules with BIK1 antibodies during any stage of division. Either BIK1 does not associate with the cytoplasmic microtubules or staining of the cytoplasmic microtubules with BIK1 antibodies is below our level of detection. Colocalization of BIK1 with tubulin was observed in cells containing the *BIK1* gene on a multicopy plasmid. Although the cytoplasmic localization of BIK1 during G1 may be the consequence of the overexpression of *BIK1*, it is unlikely that overexpression of *BIK1* affects colocalization of BIK1 with tubulin. Changes in the distribution of the BIK1 polypeptide in cells at different stages of division raise the possibility that the localization of BIK1 may be regulated during the cell cycle.

Genetic interactions between *BIK1* and the tubulin genes are consistent with the colocalization of BIK1 and tubulin. The synthetic lethality of *bik1tub1* and certain *bik1tub2* double mutants and the poor growth of others suggests that the defects in microtubule function caused by mutations in *BIK1* and the tubulin genes are additive. Similar reasoning can explain the poor growth of the *bik1 cin* double mutants. The similar phenotypes caused by mutations in the *BIK1*, *TUB*, and *CIN* genes also suggests an interaction between their products.

The BIK1 protein has structural features similar to those of the neuronal MAPs, tau and MAP2. Tau and MAP2 contain homologous regions rich in basic amino acids which bind to microtubules in vitro (Lewis et al., 1988; Lee et al., 1989) and in vivo (Lewis et al., 1989). At the amino terminus of BIK1 is a sequence that shows similarity to a segment of the microtubule binding domain of tau. This region of BIK1 as well as the entire amino-terminal region of 126 amino acids is basic, with a calculated pI of 11.3. In contrast the carboxy-terminal half of BIK1 is acidic, with a calculated pI of 4.9. Recent evidence suggests that microtubule binding may occur by electrostatic interactions between tau or MAP2 and the acidic carboxy-terminus of tubulin (Maccioni et al., 1988). These observations taken together implicate the amino terminus of BIK1 in microtubule binding.

The central and carboxy-terminal domains of BIK1 may be involved in the assembly of BIK1 into a higher order structure and its association with other cellular components, respectively. Within the central α-helical domain of BIK1 is a heptad repeat characteristic of proteins which form extended coiled-coil structures (McLachlan and Karn, 1983). The carboxy terminus of BIK1 contains a cysteine–histidine region reminiscent of "zinc fingers" (Berg, 1986). This sequence, conserved in all retroviral nucleocapsid proteins (Berg, 1986; Katz and Jentoft, 1989), is implicated in retroviral RNA packaging (Meric and Goff, 1989) and has been shown to have nucleic acid annealing activity (Prats et al., 1988; Jentoft et al., 1988). Whether this sequence in BIK1 is involved in nucleic acid binding remains to be determined.

Association of BIK1 with tubulin may promote the nucleation or assembly of microtubules, coordinating spindle formation with the cell division cycle. The cytoplasmic microtubules, absent in the *bik1* mutant, may be critical for positioning the spindle so that it elongates through the neck between mother and bud. Further studies of BIK1 may provide insight into how the formation of the mitotic spindle and cytoplasmic microtubules are temporally and spatially regulated.

We would like to thank Tim Stearns (University of California, San Francisco) for kindly providing the *cin* and *tub1* mutant strains and Tim Huffaker (Cornell University) for providing the *tub2* mutant strains. We are grateful to Frank Solomon for providing the 206.1 and 345 antitubulin antibodies. We would like to thank Jacque Fetrow (SUNY Albany) for noticing a potential metal-binding sequence in the carboxy-terminal domain of BIK1 and Alan Frankel (Whitehead Institute) for providing information regarding the metal-binding motif in retroviral nucleocapsid proteins. We are grateful to Tim Stearns and members of the laboratory for helpful discussions and to Laura Davis and Brian Keith (all from the Whitehead Institute) for critical reading of the manuscript.

This work was supported by National Institutes of Health grant GM-40266 (G. R. Fink). G. R. Fink is an American Cancer Society Professor of Genetics. V. Berlin was supported by a postdoctoral fellowship from the Jane Coffin Childs Foundation.

Received for publication 4 April 1990 and in revised form 7 August 1990.

References

Adams, A. E. M., and J. R. Pringle. 1984. Relationship of actin and tubulin distribution to bud growth in wild-type and morphogenic mutant *Saccharomyces cerevisiae*. *J. Cell Biol.* 98:934–945.

Berg, J. M. 1986. Potential metal-binding domains in nucleic acid binding proteins. *Science (Wash. DC).* 232:485–487.

Berlin, V., J. A. Brill, J. Trueheart, J. D. Boeke and G. R. Fink. 1990. Genetic screens and selections for mutants defective in cell and nuclear fusion. *Methods Enzymol.* 194:774–794.

Bloom, G. S., F. C. Luca, and R. B. Vallee. 1984. Widespread cellular distribution of MAP1A (microtubule-associated protein 1A) in the mitotic spindle and on interphase microtubules. *J. Cell Biol.* 98:331–340.

Boeke, J. D., F. Lacroute, and G. R. Fink. 1984. A positive selection for mutants lacking orotidine-5'-phosphate decarboxylase activity in yeast: 5-fluoro-orotic acid resistance. *Mol. Gen. Genet.* 197:345–347.

Borck, K., J. D. Beggs, W. J. Brammar, A. S. Hopkins, and N. E. Murray. 1976. The construction in vitro of transducing derivatives of phage lambda. *Mol. Gen. Genet.* 146:199–207.

Brown, R. S., C. Sander, and P. Argos. 1985. The primary structure of transcription factor TFIIIA has 12 consecutive repeats. *FEBS (Fed. Eur. Biochem. Soc.) Lett.* 186:271–274.

Burke, D., P. Gasdaska, and L. Hartwell. 1989. Dominant effects of tubulin over-

expression in *Saccharomyces cerevisiae*. *Mol. Cell. Biol.* 9:1049–1059.
Byers, B. 1981. Cytology of the yeast life cycle. In The Molecular Biology of the Yeast *Saccharomyces:* Life Cycle and Inheritance. J. N. Strathern, E. W. Jones, and J. R. Broach, editors. Cold Spring Harbor Laboratory, Cold Spring Harbor, NY. 59–96.
Byers, B., and L. Goetsch. 1974. Duplication of spindle plaques and integration of the yeast cell cycle. *Cold Spring Harbor Symp. Quant. Biol.* 38:123–131.
Byers, B., and L. Goetsch. 1975. Behavior of spindles and spindle plaques in the cell cycle and conjugation in *Saccharomyces cerevisiae*. *J. Bacteriol. (Lond.).* 124:511–523.
Carter, P., H. Bedouelle, and G. Winter. 1985. Improved oligonucleotide site-directed mutagenesis using M13 vectors. *Nucleic Acids Res.* 13:4431–4443.
Chou, P. Y., and G. D. Fasman. 1978. Prediction of the secondary structure of proteins from their amino acid sequence. *Adv. Enzymol.* 47:45–147.
Conde, J., and G. R. Fink. 1976. A mutant of *Saccharomyces cerevisiae* defective for nuclear fusion. *Proc. Natl. Acad. Sci. USA.* 73:3651–3655.
Dayhoff, M. O., W. C. Barker, and L. T. Hunt. 1983. Establishing homologies in protein sequences. *Methods Enzymol.* 91:524–545.
Delgado, M. A., and J. Conde. 1984. Benomyl prevents nuclear fusion in *Saccharomyces cerevisiae*. *Mol. Gen. Genet.* 193:188–189.
Franck, A., H. Guilley, G. Jonard, K. Richards, and L. Hirth. 1980. Nucleotide sequence of cauliflower mosaic virus DNA. *Cell.* 21:285–294.
Garnier, J., D. J. Osguthorpe, and B. Robson. 1978. Analysis of the accuracy and implications of simple methods for predicting the secondary structure of globular proteins. *J. Mol. Biol.* 120:97–120.
George, D. G., W. C. Barker, and L. T. Hunt. 1986. The protein identification resource (PIR) *Nucleic Acids. Res.* 14:11–15.
Gibson, T. J. 1984. Studies on the Epstein-Barr virus genome. Ph.D. thesis. University of Cambridge, Cambridge, UK.
Green, L. M., and J. M. Berg. 1989. A retroviral cys-xaa$_2$-cys-xaa$_4$-his-xaa$_4$-cys peptide binds metal ions: spectroscopic studies and a proposed three-dimensional structure. *Proc. Natl. Acad. Sci. USA.* 86:4047–4051.
Hieter, P., C. Mann, M. Snyder, and R. W. Davis. 1985. Mitotic stability of yeast chromosomes: a colony color assay that measures nondisjunction and chromosome loss. *Cell.* 40:381–392.
Hoyt, M. A., T. Stearns, and D. Botstein. 1990. Chromosome instability mutants of *Saccharomyces cerevisiae* that are defective in microtubule-mediated processes. *Mol. Cell. Biol.* 10:223–234.
Huffaker, T. C., J. T. Thomas, and D. Botstein. 1988. Diverse effects of β-tubulin mutations on microtubule formation and function. *J. Cell Biol.* 106: 1997–2010.
Ito, H., Y. Fukada, K. Murata, and A. Kimura. 1983. Transformation of intact yeast cells treated with alkali cations. *J. Bacteriol. (Lond.).* 153:163–168.
Jacobs, C. W., A. E. M. Adams, P. J. Szaniszlo, and J. R. Pringle. 1988. Functions of microtubules in the *Saccharomyces cerevisiae* cell cycle. *J. Cell Biol.* 107:1409–1426.
Jentoft, J. E., L. M. Smith, X. Fu, M. Johnson, and J. Leis. 1988. Conserved cysteine and histidine residues of avian myoblastosis virus nucleocapsid protein are essential for viral replication but are not "zinc-binding fingers." *Proc. Natl. Acad. Sci. USA.* 85:7094–7098.
Katz, R. A., and J. E. Jentoft. 1989. What is the role of the cys-his motif in retroviral nucleocapsid (NC) proteins? *Bioessays.* 11:176–181.
Kilmartin, J. 1981. Purification of yeast tubulin by self-assembly *in vitro*. *Biochemistry.* 20:3629–3633.
Kilmartin, J. V., B. Wright, and C. Milstein. 1982. Rat monoclonal antitubulin antibodies derived by using a new nonsecreting rat cell line. *J. Cell Biol.* 93:576–582.
Koerner, T. J., J. E. Hill, A. M. Myers, and A. Tzagoloff. 1990. High-expression vectors with multiple cloning sites for construction of *trpE* fusion genes: pATH vectors. *Methods Enzymol.* 194:447–490.
Laemmli, U. K. 1970. Cleavage of structural proteins during the assembly of the head of bacteriophage T4. *Nature (Lond.).* 227:680–685.
Lee, G., N. Cowan, and M. Kirschner. 1988. The primary structure and heterogeneity of tau protein from mouse brain. *Science (Wash. DC).* 239:285–288.
Lee, G., R. L. Neve, and K. S. Kosik. 1989. The microtubule binding domain of tau protein. *Neuron.* 2:1615–1624.
Lewis, S. A., D. Wang, and N. J. Cowan. 1988. Microtubule-associated protein MAP2 shares a microtubule binding motif with tau protein. *Science (Wash. DC).* 242:936–939.
Lewis, S. A., I. E. Ivanov, G. Lee, and N. J. Cowan. 1989. Organization of microtubules in dendrites and axons is determined by a short hydrophobic zipper in microtubule-associated proteins MAP2 and tau. *Nature (Lond.).* 342:498–505.
Maccioni, R. B., C. I. Rivas, and J. C. Vera. 1988. The differential interaction of synthetic peptides from the carboxy-terminal regulatory domain of tubulin with microtubule-associated proteins. *EMBO (Eur. Mol. Biol. Organ.) J.* 7:1957–1963.
Maniatis, T., E. F. Fritsch, and J. Sambrook. 1982. Molecular Cloning: A Laboratory Manual. Cold Spring Harbor Laboratory, Cold Spring Harbor, NY. 545 pp.
McLachlan, A. D., and J. Karn. 1983. Periodic features in the amino acid sequence of nematode myosin rod. *J. Mol. Biol.* 164:605–626.
Meeks-Wagner, D., J. S. Wood, B. Garvik, and L. H. Hartwell. 1986. Isolation of genes that affect mitotic chromosome transmission in *S. cerevisiae*. *Cell.* 44:53–63.
Meluh, P. B., and M. D. Rose. 1990. *KAR3*, a kinesin-related gene required for yeast nuclear fusion. *Cell.* 60:1029–1041.
Meric, C., and S. P. Goff. 1989. Characterization of Moloney murine leukemia virus mutants with single-amino acid substitutions in the cys-his box of the nucleocapsid protein. *J. Virol.* 63:1558–1568.
Miller, J., A. D. McLachlan, and A. Klug. 1985. Repetitive zinc-binding domains in the protein transcription factor IIIA from *Xenopus* oocytes. *EMBO (Eur. Mol. Biol. Organ.) J.* 4:1609–1614.
Mount, S. M., and G. M. Rubin. 1985. Complete nucleotide sequence of the *Drosophila* transposable element copia: homology between copia and retroviral proteins. *Mol. Cell. Biol.* 5:1630–1638.
Neff, N. F., J. T. Thomas, P. Grisafi, and D. Botstein. 1983. Isolation of the β-tubulin gene from yeast and demonstration of its essential function *in vivo*. *Cell.* 33:211–219.
Ohashi, A., J. Gibson, I. Gregor, and G. Schatz. 1982. Import of proteins into mitochondria. *J. Biol. Chem.* 257:13042–13047.
Olmsted, J. B. 1986. Microtubule-associated proteins. *Annu. Rev. Cell Biol.* 2:421–457.
Pearson, W. R., and D. J. Lipman. 1988. Improved tools for biological sequence comparison. *Proc. Natl. Acad. Sci. USA.* 85:2444–2448.
Polaina, J., and J. Conde. 1982. Genes involved in the control of nuclear fusion during the sexual cycle of *Saccharomyces cerevisiae*. *Mol. Gen. Genet.* 186:253–258.
Prats, A. C., L. Sarih, C. Gabus, S. Litvak, G. Keith, and J. L. Darlix. 1988. Small finger protein of avian and murine retroviruses has nucleic acid annealing activity and positions the replication primer tRNA onto genomic RNA. *EMBO (Eur. Mol. Biol. Organ.) J.* 7:1777–1783.
Quinlan, R. A., C. I. Pogson, and K. Gull. 1980. The influence of the microtubule inhibitor methyl benzimidazol-2-yl-carbamate (MBC) on nuclear division and the cell cycle in *Saccharomyces cerevisiae*. *J. Cell Sci.* 46:341–352.
Rose, M. D., and G. R. Fink. 1987. *KAR1*, a gene required for function of both intranuclear and extranuclear microtubules in yeast. *Cell.* 48:1047–1060.
Rose, M. D., L. Misra, and J. P. Vogel. 1989. *KAR2*, a karyogamy gene, is the yeast homolog of mammalian BiP/GRP78 gene. *Cell.* 57:1211–1221.
Rothstein, R. J. 1983. One-step gene disruption in yeast. *Methods Enzymol.* 101:202–211.
Schatz, P. J., L. Pillus, P. Grisafi, F. Solomon, and D. Botstein. 1986*a*. Two functional α-tubulin genes of the yeast *Saccharomyces cerevisiae* encode divergent proteins. *Mol. Cell Biol.* 6:3711–3721.
Schatz, P. J., F. Solomon, and D. Botstein. 1986*b*. Genetically essential and nonessential α-tubulin genes specify functionally interchangeable proteins. *Mol. Cell. Biol.* 6:3722–3733.
Schatz, P. J., F. Solomon, and D. Botstein. 1988. Isolation and characterization of conditional-lethal mutations in the *TUB1* α-tubulin gene of the yeast *Saccharomyces cerevisiae*. *Genetics.* 120:681–695.
Sherman, F., J. B. Hicks, and G. R. Fink. 1986. Methods in Yeast Genetics. Cold Spring Harbor Laboratory, Cold Spring Harbor, NY. 163–167.
Sikorski, R. S., and P. Hieter. 1989. A system of shuttle vectors and yeast host strains designed for efficient manipulation of DNA in *S. cerevisiae*. *Genetics.* 122:19–27.
South, T. L., B. Kim, and M. F. Summers. 1989. ^{113}Cd NMR studies of a 1:1 adduct with an 18-residue finger peptide from HIV-1 nucleic acid binding protein, p7. *J. Am. Chem. Soc.* 111:395–396.
Southern, E. M. 1975. Detection of specific sequences among DNA fragments separated by gel electrophoresis. *J. Mol. Biol.* 98:503–517.
Stearns, T., and D. Botstein. 1988. Unlinked noncomplementation: isolation of new conditional-lethal mutations in each of the tubulin genes of *Saccharomyces cerevisiae*. *Genetics.* 119:249–260.
Stearns, T., M. A. Hoyt, and D. Botstein. 1990. Yeast mutants sensitive to antimicrotubule drugs define three genes that regulate microtubule function. *Genetics.* 124:251–262.
Struhl, K. 1983. Direct selection for gene replacement events in yeast. *Gene (Amst.).* 26:231–242.
Suissa, M. 1983. Spectrophotometric quantitation of silver grains eluted from autoradiograms. *Anal. Biochem.* 133:511–514.
Thomas, J. T. 1984. Genes controlling the mitotic spindle and chromosome segregation in yeast. Ph.D. thesis. Massachusetts Institute of Technology, Cambridge, MA.
Thomas, J. T., N. F. Neff, and D. Botstein. 1985. Isolation and characterization of mutations in the β-tubulin gene of *Saccharomyces cerevisiae*. *Genetics.* 111:715–734.
Trueheart, J., J. D. Boeke, and G. R. Fink. 1987. Two genes required for cell fusion during yeast conjugation: evidence for α pheromone-induced surface protein. *Mol. Cell. Biol.* 7:2316–2326.
Vallee, R. B., and G. S. Bloom, 1983. Isolation of sea urchin egg microtubules using taxol and identification of mitotic spindle MAPs with the use of monoclonal antibodies. *Proc. Natl. Acad. Sci. USA.* 80:6259–6263.
Wood, J. S., and L. H. Hartwell. 1982. A dependent pathway of gene functions leading to chromosome segregation in *Saccharomyces cerevisiae*. *J. Cell Biol.* 94:718–726.
Yanisch-Perron, C., J. Viera, and J. Messing. 1985. Improved M13 phage cloning vectors and host strains: nucleotide sequences of the M13mp18 and pUC19 vectors. *Gene (Amst.).* 33:103–119.